AGU ADVANCING EARTH AND SPACE SCIENCES

Geophysical Research Letters

RESEARCH LETTER

10.1029/2024GL111939

Infiltration Dynamics on Early Mars: Geomorphic, Climatic, and Water Storage Implications

Mohammad Afzal Shadab[1,2,3,4], **Eric Hiatt**[2,3,5], **Rickbir Singh Bahia**[6], **Eleni V. Bohacek**[6], **Vilmos Steinmann**[7,8], **and Marc Andre Hesse**[1,5]

[1]Oden Institute for Computational Engineering and Sciences, The University of Texas at Austin, Austin, TX, USA, [2]University of Texas Institute for Geophysics, The University of Texas at Austin, Austin, TX, USA, [3]Center for Planetary Systems Habitability, The University of Texas at Austin, Austin, TX, USA, [4]Department of Civil and Environmental Engineering, Princeton University, Princeton, NJ, USA, [5]Department of Earth and Planetary Sciences, The University of Texas at Austin, Austin, TX, USA, [6]European Space Research and Technology Centre (ESTEC), Noordwijk, The Netherlands, [7]Eötvös Loránd University, Budapest, Hungary, [8]Konkoly Thege Miklós Astronomical Institute, Research Centre for Astronomy and Earth Sciences, Budapest, Hungary

Key Points:

- Infiltration leads to less ponded water and more aeolian erosion, and its rate dynamically decays with time due to subsurface heterogeneity
- Deep crustal infiltration takes decades to recharge groundwater system, delaying aquifer response and storing significant amount of water
- This simple infiltration model enables fast and more accurate groundwater and surface modeling while also providing a link between both

Supporting Information:

Supporting Information may be found in the online version of this article.

Correspondence to:

M. A. Shadab,
mashadab@princeton.edu

Citation:

Shadab, M. A., Hiatt, E., Bahia, R. S., Bohacek, E. V., Steinmann, V., & Hesse, M. A. (2025). Infiltration dynamics on early Mars: Geomorphic, climatic, and water storage implications. *Geophysical Research Letters*, *52*, e2024GL111939. https://doi.org/10.1029/2024GL111939

Received 11 AUG 2024
Accepted 17 MAR 2025

Author Contributions:

Conceptualization: Mohammad Afzal Shadab, Eric Hiatt, Rickbir Singh Bahia, Eleni V. Bohacek, Vilmos Steinmann, Marc Andre Hesse
Data curation: Mohammad Afzal Shadab
Formal analysis: Mohammad Afzal Shadab, Eric Hiatt, Rickbir Singh Bahia, Eleni V. Bohacek
Funding acquisition: Mohammad Afzal Shadab, Marc Andre Hesse
Investigation: Mohammad Afzal Shadab
Methodology: Mohammad Afzal Shadab, Eric Hiatt, Rickbir Singh Bahia, Eleni V. Bohacek, Marc Andre Hesse
Project administration: Mohammad Afzal Shadab

Abstract

On early Mars, the integration of surface, groundwater, and climate systems into an integrated hydrological system remains poorly understood. The partitioning of precipitation, between surface and groundwater via infiltration, controls the Martian aquifer recharge rates and, subsequently, surface erosion processes. We investigate infiltration at two scales, near-surface and deep crustal. We estimate infiltration timescales, revealing that near-surface water loss enhances aeolian erosion over short periods (hours to days). Deep crustal recharge, which requires decades to centuries, affects the deep aquifer response and the water budget. Martian crustal heterogeneity influences infiltration dynamics and runoff production making them dependent on the duration of precipitation. This interaction suggests that the responses of the aquifers to recharge events and groundwater upwelling likely lag behind climate optimum conditions. The accommodation space between topography and aquifer influences Mars' water budget by transiently sequestering water, thus limiting the available water for surface evaporation and inclusion in climate dynamics.

Plain Language Summary

Early Mars experienced occasional periods of active surface water and groundwater processes. However, details on how surface, groundwater, and climate processes interact to form a complete water cycle are still unclear. Specifically, the dynamics of the process by which precipitation either infiltrates into the subsurface or forms surface runoff are poorly understood. This division controls the water volume and time scales associated with the recharge of early Martian aquifers, and the surface water runoff that forms lakes and basins. We investigated the infiltration dynamics and calculated how long it takes for water to seep into Mars' shallow and deep subsurface. We found that heterogeneities in the subsurface lead to an evolving infiltration rate that changes with time. It is not a static rate as assumed earlier in previous work. In addition, the region between the surface and the deep aquifer, called the vadose zone, can transiently accommodate a significant amount of groundwater that has not been accounted for in prior studies.

1. Introduction

In its current state, Mars is cold and arid (Haberle et al., 2017). However, remotely sensed and in situ geomorphic observations provide clear evidence of past surface water activity (e.g., Ehlmann et al., 2011; Fassett & Head, 2008; Grotzinger et al., 2014; Hynek et al., 2010; Manga & Wright, 2021; Squyres et al., 2004). Abundant evidence for past surface water activity naturally implies the existence of associated groundwater systems, and these systems have been suggested in prior studies (e.g., Andrews-Hanna et al., 2007, 2010; Clifford, 1993; Clifford & Parker, 2001; Hiatt et al., 2024; Horvath & Andrews-Hanna, 2017; Luo & Howard, 2008; Malin & Edgett, 2000; Salese et al., 2019). However, the connections between climate, groundwater, and surface water processes, into an integrated hydrological system on early Mars, remain poorly understood.

There are multiple processes by which water is partitioned into an integrated hydrological system (Boatwright & Head, 2019) that have been extensively studied in terrestrial hydrological systems (e.g., Cherry & Freeze, 1979; Gee & Hillel, 1988; Scanlon et al., 2006). Infiltration is one such process that occurs when precipitation percolates into the subsurface of a planet. Another process, runoff production, is defined as the percentage of the precipitation that does not infiltrate the subsurface or evaporate into the atmosphere and acts to move water to basins

Resources: Mohammad Afzal Shadab
Software: Mohammad Afzal Shadab
Supervision: Mohammad Afzal Shadab
Validation: Mohammad Afzal Shadab
Visualization: Mohammad Afzal Shadab
Writing – original draft: Mohammad Afzal Shadab, Eric Hiatt
Writing – review & editing: Mohammad Afzal Shadab, Eric Hiatt, Rickbir Singh Bahia, Eleni V. Bohacek, Vilmos Steinmann, Marc Andre Hesse

where it can eventually be infiltrated, evaporated, or stored. Lastly, evaporation occurs when surface water is evaporated back into a planet's atmosphere and into the climate system. Together, these processes determine the partitioning of available water between climate, surface, and groundwater systems in an integrated hydrological cycle. The dynamics associated with these processes are dictated by the interplay of numerous factors such as the areal distribution of precipitation, climate conditions (aridity and temperature controls on evaporation), topography (determines where runoff will produce basins) and elevations of the groundwater table (affects the total volume and variable rate of infiltration).

To gain insight into the integrated hydrological cycle of early Mars, we chose to focus on infiltration rates into the shallow and deep Martian crust. In hydrological models, precipitation rates are specified by global climate model solutions. These models are outside the scope of this work. When a specified precipitation rate is applied to the surface of a planet, the maximum rate of infiltration dictates the percentage of precipitation that remains to produce runoff. This dependence on infiltration makes analyzing the dynamics of this process an attractive method to explore the connections between surface water, groundwater, and climate systems on early Mars.

Infiltration processes would have played an important role in the hydrological processes of ancient Mars, similar to the role of infiltration in terrestrial desert environments (e.g., Jarihani et al., 2015; Mathias et al., 2021). However, this dynamic process is generally ignored in land evolution models (Boatwright & Head, 2019). Similarly, dynamic infiltration is often ignored in groundwater studies on both global and regional scales (e.g., Andrews-Hanna et al., 2010; Hiatt et al., 2024; Horvath & Andrews-Hanna, 2017, 2021). When infiltration is considered in models, it is assumed to be a constant that linearly affects runoff production (Boatwright & Head, 2019). In this work, we will show that a constant infiltration rate defined for a homogeneous regolith is an oversimplification, and the dependence is the converse.

Quantifying and accounting for infiltration rates as a dynamic process has important implications for the partitioning of water between systems. Generally, infiltration rates become nonlinear due to decreased hydraulic conductivity caused by permeability and porosity decay with depth, at large global groundwater scales, and at shallow groundwater scales, heterogeneity in the vadose zone and regolith cause nonlinear changes in hydraulic conductivity and subsequent infiltration. As groundwater infiltrates areas with lower permeability in the shallow subsurface and deep crust, a nonlinear decrease in infiltration rates will cause a nonlinear increase in runoff production (Beven, 1984; Green & Ampt, 1911; Kale & Sahoo, 2011; Mein & Larson, 1973; Selker et al., 1999; Shadab & Hesse, 2022). This implies that runoff production is a dynamic function of variable infiltration rates, which is a function of the location of the wetting front that separates relatively dry and wet regions in the subsurface, as well as a function of the precipitation rate and the duration of the climate conditions that produce precipitation events. In an integrated hydrological system, variance in runoff rates would then affect the surface water ponding by controlling the volume available to be ponded and stored. This is consequential because the water within a basin can become a source of evaporation for the climate system, as well as a localized source for infiltration into the groundwater system.

We demonstrate that the models (Boatwright & Head, 2019; Hanna & Phillips, 2005; Shadab et al., 2023, e.g.) for permeability and porosity decay with depth that are commonly used in groundwater studies produce diminishing recharge rates as the wetting front percolates downward. This diminishing infiltration rate would enhance surface runoff that is unaccounted for, leading to inaccuracies in land evolution models. Downward percolation implies that the depth of the groundwater table below the topography also becomes an important variable in an integrated hydrological cycle on early Mars. On geologic time scales, it is likely that the early Mars climate would only produce short-duration, transient precipitation events (Salese et al., 2020; Wordsworth, 2016), and the groundwater table would have likely been below the surface during arid intervals (Hiatt et al., 2024). The greater the depth to the deep groundwater table, the greater the reduction in infiltration rate.

An additional implication of detached surface and groundwater systems that has not been considered in the literature is the considerable volume of accommodation space within the empty pore space contained in the crust between the topography and the water table. We show that the volume of water capable of being stored is significant when compared to estimates of water availability. This has implications for the availability of surface water to evaporate and then precipitate within the climate system. Lastly, the depth to the groundwater table affects the time interval required to percolate from the topography to the water table. This time interval would have delayed the response of the groundwater table to recharge, which is ignored in contemporary groundwater

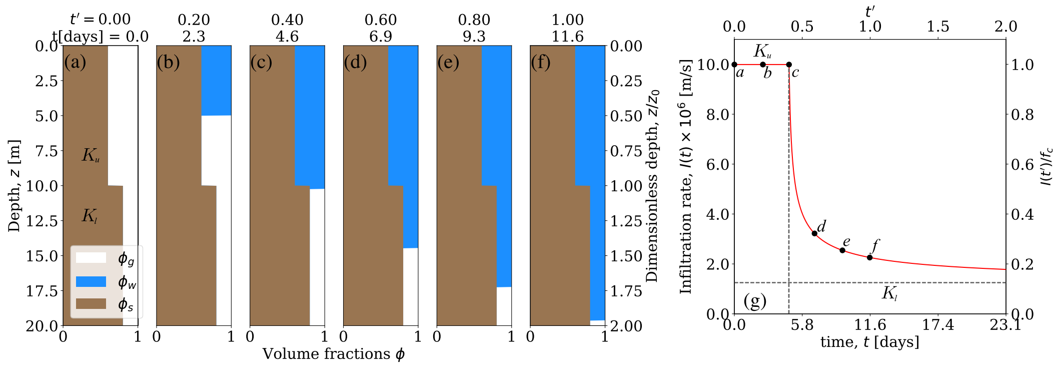

Figure 1. Near-surface infiltration on early Mars: (a–f) Infiltration in 10 m deep sand dunes lying on top of cemented sand due to ponded infiltration. The volume fraction ϕ_α is the ratio of the volume occupied by α phase to the bulk volume where α can be gas (g), water (w), and regolith (s). (g) Evolution of corresponding infiltration rate I (or transmission loss). The dimensionless variables are also provided for the sake of generality.

models (e.g., Andrews-Hanna et al., 2007, 2008; Boatwright & Head, 2019; Hiatt et al., 2024; Luo & Howard, 2008).

Infiltration clearly affects the integration of the hydrological cycle on early Mars. In this work, we examine the dynamic processes of infiltration analytically. Quantifying the time scales associated with percolation, transient infiltration rates, and the pore volume capable of sequestering water will allow analysis and numerical models to incorporate infiltration as a dynamic process. This work seeks to answer two fundamental questions; What was the dynamic role of infiltration in the early Mars hydrosphere and how can we incorporate these findings in future work?

2. Infiltration Model

Here we consider infiltration produced by ponded water referred to as percolation-limited infiltration (Shadab & Hesse, 2022). We assume that a ponded layer is sufficiently thin and that the capillary effects are negligible compared to gravitational effects, similar to Boatwright and Head (2019). This assumption is a good approximation at large spatial scales or in a low-textured regolith, such as sand (Shadab & Hesse, 2022). However, unlike Boatwright and Head (2019), the subsurface is assumed to be heterogeneous with a decay in conductivity with depth. The flux of water transmitted to the subsurface is defined as infiltration rate $I(t)$, in a porous media (m^3/m^2s) with porosity ϕ and hydraulic conductivity K (m/s) decaying or remaining constant with depth z (m), which is given by

$$I(t) = \frac{z_l}{\int_0^{z_l} \mathrm{d}z/K(z)} \quad \text{with} \quad \frac{\mathrm{d}z_l}{\mathrm{d}t} = \frac{I(t)}{\phi(1 - s_{wr} - s_{gr})} \tag{1}$$

where z_l is the depth of the wetting front with respect to the surface (m) and s_{wr} and s_{gr} are the residual saturations (fraction occupied in the pore space) of water and gas phases respectively. The above model is non-dimensionalized in Text S2 in Supporting Information S1 by picking a characteristic length scale z_0 and time scale z_0/f_c to provide results for a class of regolith properties with variable characteristic depths and infiltration capacities f_c. For infiltration due to a thin ponded layer in the absence of capillary forces, the infiltration capacity f_c is identical to surface hydraulic conductivity $K(z = 0)$, which is a constant. The conversion from dimensionless to dimensional variables provides a crucial handle to estimate time scales, given variable-length scales and regolith types. This allows the choice of any thickness or infiltration capacity (i.e., surface hydraulic conductivity) of dune layers/crust that best describes the geologic conditions being studied, considering the lack of direct/indirect measurements. For the characteristic depth z_0 with an infiltration capacity of f_c, the characteristic time scale is z_0/f_c. In the figures, we also show the dimensionless variables for generality.

For shallow subsurface, we consider infiltration into a 10 m deep sand dune ($\phi = 0.4$, $K_u = f_c = 10^{-5}$ m/s) overlying cemented sand ($\phi = 0.2$, $K_l = 1.56 \cdot 10^{-6}$ m/s), as shown in Figure 1a, that effectively simulates a

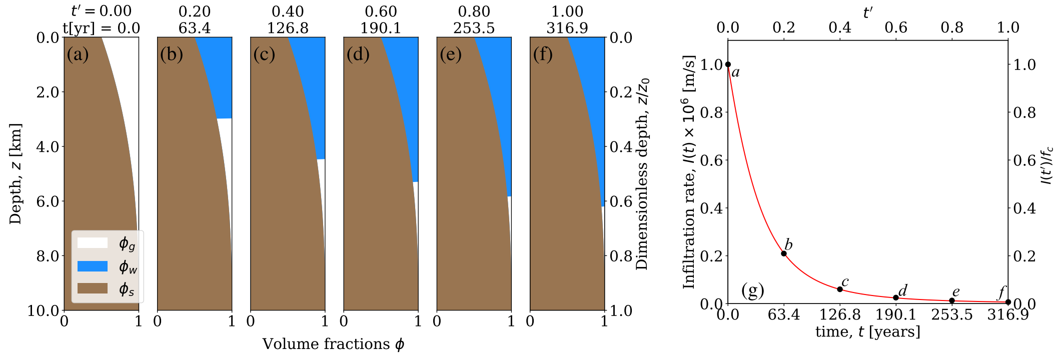

Figure 2. Infiltration into 10 km deep crust on early Mars due to ponded infiltration. Here the volume fraction ϕ_α is defined for each α: gas (g), water (w), and regolith (s). (g) Evolution of corresponding infiltration rate I (or transmission loss). The dimensionless variables are also provided for the sake of generality.

double-textured, special type of regolith configuration with a coarse-to-fine transition at depth $z_0 = 10$ m. The analytic solutions for the wetting front location and infiltration rate for a two-layer regolith configuration are provided in Text S2.2.1 in Supporting Information S1.

On a crustal scale, the porosity and conductivity can be assumed to decay with depth (Clifford & Parker, 2001; Hanna & Phillips, 2005; Manning & Ingebritsen, 1999) as

$$\phi(z) = \phi_0(1 - z/z_0)^{\mathrm{p}} \quad \text{and} \quad K(z) = K_0(1 - z/z_0)^{\mathrm{p}m} \tag{2}$$

where ϕ_0 is the constant porosity at the surface, z_0 is the depth to the impermeable bedrock where $\phi = 0$ and p is the empirically calculated power-law exponent (Figure 2a).

We define a new variable, infiltration time t_{inf}, as the time taken by the wetting front to reach the groundwater table after entering the subsurface. Infiltration times can be calculated from Equation 1 for a homogeneous crust as

$$t_{\mathrm{inf}} = \left(\frac{z_{\mathrm{surf}} - z_{\mathrm{GW}}}{f_c}\right)\phi_0(1 - s_{gr} - s_{wr}) \tag{3}$$

and for a heterogeneous crust as

$$t_{\mathrm{inf}} = \mathcal{I}\left(m, \mathrm{p}, \frac{z_{\mathrm{surf}} - z_{\mathrm{GW}}}{z_{\mathrm{surf}} - z_{\mathrm{base}}}\right)\frac{1}{m\mathrm{p} - 1}\left(\frac{z_{\mathrm{surf}} - z_{\mathrm{base}}}{f_c}\right)\phi_0(1 - s_{gr} - s_{wr}), \tag{4}$$

where f_c is the infiltration capacity or the hydraulic conductivity at the surface (m/s), that is, $K(0)$, z_{surf} is the elevation of the surface topographic elevation (m), z_{GW} is the elevation of the groundwater table (m), z_{base} is the elevation of the impermeable base here set at $z_{\mathrm{base}} = -9000$ m. Furthermore, $\mathcal{I}(m, \mathrm{p}, z'_{\mathrm{GW}})$ is a dimensionless integral function defined by $\mathcal{I}(m, \mathrm{p}, z'_{\mathrm{GW}}) = \int_0^{z'_{\mathrm{GW}}} \frac{(1-z')^{\mathrm{p}-m\mathrm{p}+1} - (1-z')^{\mathrm{p}}}{z'} \mathrm{d}z'$. This function can be evaluated numerically for a dimensionless water table depth $z'_{\mathrm{GW}} \in [0, 1]$ once the power law exponents p and m are defined. Here, the depth of the impermeable bedrock at each location is $z_0 = z_{\mathrm{surf}} - z_{\mathrm{base}}$. We used the results of the deep unconfined aquifer model from Hiatt et al. (2024) to make estimates of z_{GW} at each raster location and the Mars Orbiter Laser Altimeter (Smith et al., 2001) topography data to estimate z_{surf}. Note that unlike the groundwater models that measure properties as a function of elevation above bedrock, this infiltration model utilizes depth below the surface. As a result, the porosity and permeability at two different raster locations with the same height above the bedrock will be identical only if the surface to bedrock depths are the same. In this study, we assume the bedrock to be impermeable, which could also be considered the base of the aquifer. For the basaltic crust with a power law decay (Manning & Ingebritsen, 1999), we pick the surface porosity to be $\phi_0 = 0.5$ and extract the conductivity at the surface to be approximately $K_0 = 10^{-6}$ m/s and the exponents to be $\mathrm{p} = 2.5422$

10.1029/2024GL111939

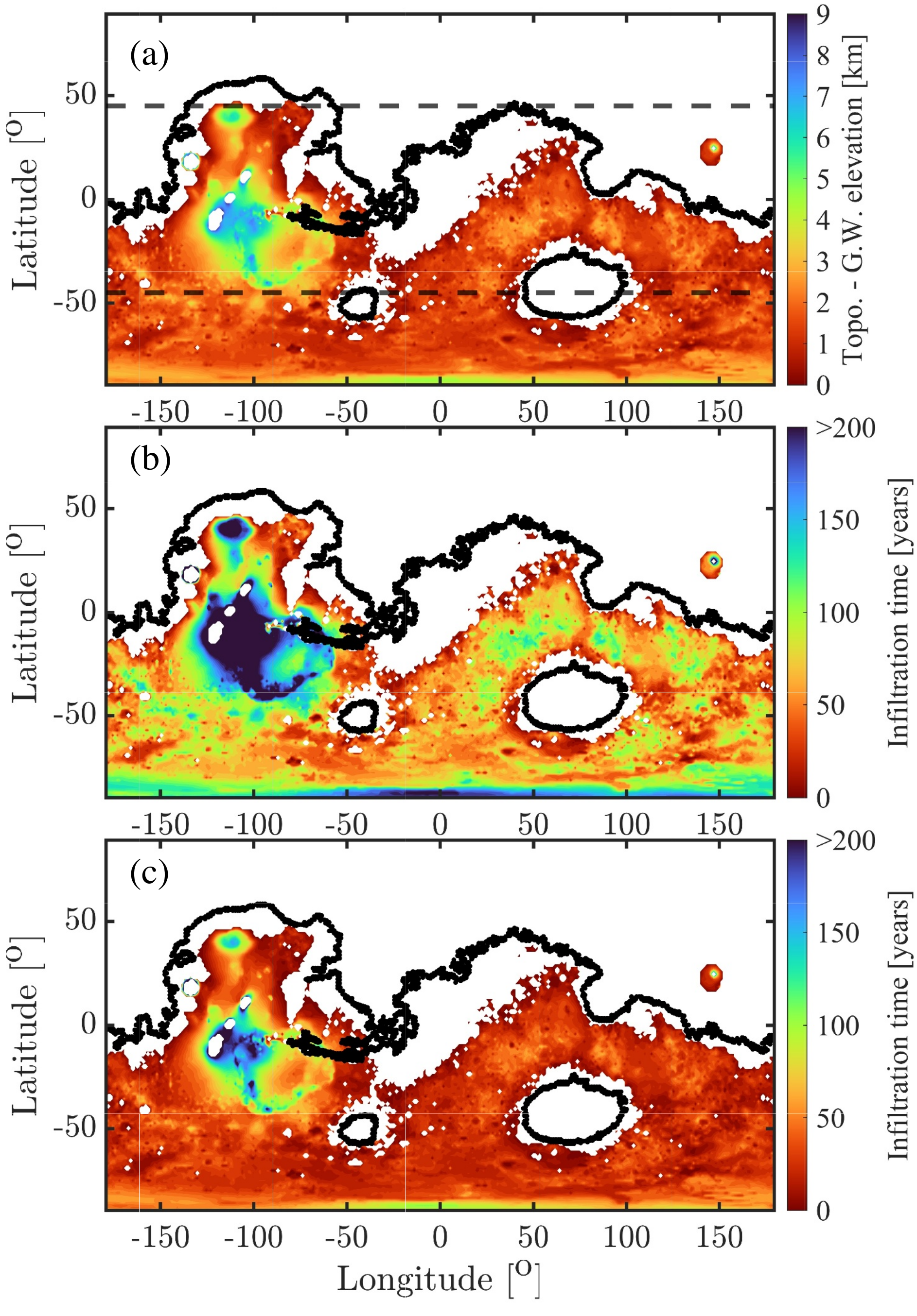

Figure 3. Infiltration on early Mars. (a) Difference in elevation of the topography and water table $z_{\mathrm{surf}} - z_{\mathrm{GW}}$ (m). The steady groundwater table has resulted from a banded recharge of 10 μm/year in between −45°S to 45°N (black dashed line) with Arabia shoreline at −2,090 m elevation, including in Hellas and Argyre, all shown with solid black lines. (b) Infiltration time for homogeneous crust with uniform hydraulic conductivity of $f_c = 10^{-7}$ m/s and porosity of $\phi_0 = 0.1412$. (c) Infiltration time for heterogeneous crust with power-law decay in porosity and permeability with surface values $\phi_0 = 0.5$ and $f_c = 10^{-6}$ m/s. The power law exponents are given in the main text. Infiltration time refers to the time elapsed for surface water to reach the groundwater table. White space on the map refers to water already present at or near surface, not considered in the present study.

and $m = 3$ (Figure 2a). Text S3 in Supporting Information S1 provides the power-law fits to the porosity using Clifford and Parker (2001) and permeability/hydraulic conductivity with depth using Manning and Ingebritsen (1999), instead of exponential decay because it fails to decay to zero at the bedrock (Shadab et al., 2023). We chose $s_{wr} = s_{gr} = 0$ for simple estimations of infiltration times. In addition, we used an equivalent homogeneous aquifer with vertically averaged values in Figure 3b with $\phi_0 = 0.1412$ and $K_0 = 10^{-7}$ m/s to consider the effects of vertical heterogeneity. In the discussion section, the amount of pore space available is calculated as a Global Equivalent Layer (GEL, in m). Text S1 in Supporting Information S1 describes the theory and implementation used to calculate GEL equivalent that can be transiently stored in the vadose zone.

2.1. Implementation of Infiltration Dynamics in Groundwater and Geomorphological Models

Finally, we provide the steps to implement the proposed infiltration model in standard groundwater and land evolution models. The purpose of this section is to improve the accessibility of the proposed model for future research. The amount of water lost to the subsurface can be taken into account in geomorphic and groundwater models. At each raster location, a new function can be implemented in existing codes to estimate infiltration. This function tracks the instantaneous infiltration rate $I(t)$ and the location of the wetting front z_l. The infiltration rate can be calculated (semi-)analytically by solving Equation 1 after substituting the porosity and permeability definitions (Equation 2) for the time-varying infiltration rate $I(t)$ and the location of the wetting front $z_l(t)$. These analytic values and associated codes are provided in Text S2 in Supporting Information S1 (taken from Shadab and Hesse (2022)) and on Github (Shadab & Hesse, 2022; Shadab et al., 2025) respectively for standard porous media and regolith conditions, including double layer, and exponential and power law decay in porosity and permeability with depth. The amount of water lost to the subsurface is the product of the infiltration rate, the surface area of the raster, and the time step. Once calculated, the water volume can be subtracted from the surface water volume in the raster until the water that can be infiltrated is exhausted. Using this method, Martian hydrologists and modelers could easily incorporate this first-order estimate of water loss due to infiltration into existing and future models.

To implement infiltration in groundwater models, there are two scenarios to consider. If the time-step interval of the groundwater model is greater than the calculated infiltration time, the infiltration process can be ignored. However, if the infiltration time is greater than the duration of the time step, the delay due to infiltration should be considered. Once the wetting front reaches the water table, the groundwater table could be set to the surface, if recharge is still ongoing, or the elevation of the groundwater table then becomes the elevation of the surface topography. It will lead to lateral hydraulic gradients within the aquifer and affect the heights of the water table, thus affecting the infiltration time. Once the ponded layer becomes negligible with no infiltration, the height of the water table could be released and allowed to numerically evolve by itself.

3. Results

The model described in Section 2 can be used to simulate infiltration on early Mars. In Figures 1a–1f, we simulate shallow infiltration into a 10 m deep sand dune overlying cemented sand. Initially, the front propagates at a relatively fast and constant velocity in the highly conductive top layer of the sand dune until $t < 4.6$ days ($t' < 0.4$) (Figures 1a–1c). The infiltration rate $I(t)$ remains constant during this process, due to the initial lack of heterogeneity in the subsurface experienced by the wetting front (Figure 1g). However, after the front reaches the transition depth $z_0 = 10$ m ($z/z_0 = 1$) at $t = 4.6$ days ($t' = 0.40$), the front speed decreases sharply due to the reduced ability of the lower layer to accommodate flow (Figure 1c). This also leads to a sharp reduction in the infiltration rate which results in an increased ponding of water at the surface. In addition, the infiltration rate gradually decreases according to the conditions experienced in the decelerating wetting front as the front moves within the lower layer of cemented sand (Figure 1g). In the late stages ($t \gg 4.6$ days), the dynamics are predominantly governed by the lower regolith layer with the infiltration rate gradually declining asymptotically to its saturated hydraulic conductivity K_l (Figures 1f and 1g). For the transition depth z_0 of 10 m with an infiltration capacity of $f_c = K_u = 10^{-5}$ m/s, $t' = 1$ is equivalent to $z_0/f_c = 11.6$ days. Thus, dunes with transition depths z_0 of 1 and 20 m will take 1.2 and 23.2 days, respectively, for the transition. These time scales can be calculated by redimensionalizing dimensionless time $t' = 1$ to dimensional time t using $t = t' z_0/f_c$ using corresponding characteristic depth z_0 and infiltration capacity f_c.

Figures 2a–2f show the deep infiltration into the Martian crust assumed to have a continuous, power-law decay in porosity and conductivity. At the characteristic depth of $z_0 = 10$ km ($z/z_0 = 1$), the porosity and conductivity both decay to zero, that is, the crust becomes impermeable. The infiltration rate (Figure 2g) rapidly decays due to a vertical heterogeneity experienced by the wetting front, leading to a decelerating wetting front. This ultimately

10.1029/2024GL111939

leads to a decreased transmission loss rate of the surface ponded water at longer times. The basaltic crust with surface hydraulic conductivity or in this case the infiltration capacity $f_c = 10^{-6}$ m/s, and the impermeable bedrock depth $z_0 = 10$ km, $t' = 1$ corresponds to $t = z_0/f_c = 316.88$ years. For an initial period, there is a significant reduction in surface water lost to the subsurface. In a span of about 126.8 years $(t' = 0.4)$, the transmission loss is reduced to less than 1/10th of its initial value ($I \sim 10^{-6}$ m/s). It underscores the importance of considering the heterogeneity in the crust. If the water table exists at about 2–5 km depth $(z' = 0.2 - 0.5)$, it will take about 50–200 years for the wetting front to reach the global groundwater table (Figures 2b–2d).

Lastly, we study deep infiltration in the southern highlands on early Mars with a steady groundwater table determined using a deep groundwater aquifer model (Hiatt et al., 2024). The steady groundwater model assumed a cosine variation in the distribution of aquifer recharge. This variance was centered on the equator in a band of −45°S to 45°N. The assumed recharge rate was 10 μm/year. This leads to a steady groundwater table below much of the topography (Figure 3a, see figure caption for more information). The regolith in the vadose zone, between the topographic surface and the saturated groundwater table, is considered dry. This simplification helps make estimates of the time required for the surface water to reach the subsurface via infiltration, referred to as infiltration time. Here we consider two types of crust, a heterogeneous crust with a power-law decay (Figure 3c) and an equivalent homogeneous crust (Figure 3b), to highlight the effect of vertical heterogeneity. For a uniform basaltic crust, it takes almost a century (85.16 ± 37.58 years) for surface water to reach the steady water table in most of the southern highlands (Figure 3b). The infiltration time increases to several centuries in the Tharsis region due to its increased elevation. Here we do not assume surface flow, but we intend to make the first estimates of the time elapsed. For a heterogeneous crust, the average infiltration time decreases to several decades (37.58 ± 32.07 years, Figure 3c), as estimated previously in Figure 2. This occurs as the water table is relatively closer to the surface in the majority of highlands, that is, within about 10%–20% of the surface-to-bedrock depth (Figures S3a and S3b in Supporting Information S1) where the porosity and hydraulic conductivity are higher than that for the homogeneous crust leading to faster wetting fronts.

4. Discussion

Infiltration processes are key to understanding the dynamics associated with an integrated hydrological cycle at both the shallow subsurface and deep crustal scales. At the deep crust scale, ignored or poorly constrained infiltration rates would not account for a delay in the transient aquifer response due to percolation time scales nor would it account for the effects of vadose zone pore storage space that will transiently sequester water. At the shallow crust scale, ignoring or poorly constraining infiltration rates would lead to overestimates of water-related processes, misinterpretations of hydrological and climatic history, and inaccuracies in understanding the formation and evolution of geomorphic features. No model incorporates a temporally dynamic infiltration rate described in this work.

Land evolution models that ignore water loss due to infiltration will produce an overestimation of water availability and inaccurate predictions regarding the volume and duration of Martian paleolakes, rivers, and other surface water bodies. These inaccuracies affect the models' predictions. Furthermore, overestimated runoff volumes would suggest higher erosion rates and higher sediment transport capacities. These overestimations are produced by sharp transitions in regolith permeability such as aeolian-to-megaregolith transitions, as well as deeper megaregolith-to-bedrock transitions. As the wetting front encounters these sharp transitions in permeability, the speed at which the front can propagate downward is diminished, which then affects the maximum rate of infiltration at the surface. This transient rate of infiltration underscores the nature of precipitation partitioning processes, as downward percolation of the wetting front produces increased runoff. At the shallow crust scale, infiltration processes affect geomorphology through surface water losses, leading to reduced surface water ponding. Models that do not account for this decrease in surface water are modeling geomorphological processes with excess water. A regolith with decreased antecedent moisture will lead to more erosion due to lack of cohesion and increased aeolian effects. However, there may be a concomitant decrease in erosion due to runoff because infiltration will decrease the volume of water available for runoff processes. However, in models other than MARSSIM, the precipitation rate is equivalent to the production of runoff (Howard, 1994; Pelletier, 2008; Tucker & Hancock, 2010).

Land evolution models that consider infiltration as a linear process still produce inaccuracies with a non-dynamical approach. The MARSSIM landform evolution model assumes either complete runoff/infiltration or mixed infiltration-runoff in a homogeneous regolith (Boatwright & Head, 2019). In the shallow subsurface, MARSSIM utilizes the Green and Ampt (1911) model by assuming a constant hydraulic conductivity $K = 3.1 \cdot 10^{-6}$ m/s. However, its deep groundwater aquifer model assumes a heterogeneous subsurface with hydraulic conductivity that decays exponentially with depth calculated with the Manning and Ingebritsen (1999) method. The MARSSIM model is the only model the authors are aware of that attempts to implement infiltration dynamics, however, MARSSIM only roughly addresses infiltration by assuming that surface water loss occurs at a constant infiltration rate without considering the hydrology of the vadose zone. Even though MARSSIM is more advanced than other models, this approach is unable to examine the effects of vadose zone hydrology and the distribution of water within the vadose zone. As a result, MARSSIM may incur large errors in surface water losses, basin water volume calculations, and deep aquifer recharge rates due to the use of a non-dynamic infiltration rate. However, MARSSIM could be easily updated with the infiltration dynamics described in this work and thus provides an excellent tool for future work interrogating these effects.

Effects from the climate system will also complicate the partitioning of water. As the climate conditions that produce precipitation events evolve, the duration of the precipitation event affects the extent of fluvial erosion. Short-duration precipitation events allow a greater percentage of precipitated water to infiltrate the subsurface due to the high initial infiltration rates. However, for longer-duration storms, the infiltration, or transmission loss, rate will decay over time due to the downward percolating wetting front interacting with the less permeable layer(s) at depth (Figure 1g). These temporal dependencies are further compounded by partitioning variations due to changes in precipitation rate and the timing of the rate of oscillations within the precipitation event.

This work provides a method for including dynamic infiltration in land evolution models. These rates can include the effects of heterogeneities in the subsurface which will improve model accuracy. However, this method also provides another valuable function. The proposed infiltration model can be a method for linking land evolution and groundwater models. Thus, the implementation of the present infiltration model in Mars land evolution models such as MARSSIM and groundwater models will allow for a more accurate determination of overall water partitioning and landform evolution in future investigations.

As discussed previously, dynamic infiltration can affect the volume of water entering a basin. Paleolakes within basins would have lost water to the subsurface orders of magnitude faster than losses to the atmosphere through evaporation. These basins would lose water to the subsurface in the same dynamical way surface water would; however, it could be a sustained source of recharge for the groundwater system. Paleolake studies should assume infiltration when predicting the lifetime of surface water. This increased runoff may produce an accumulation of surface water in basins that could act as regional point sources of increased infiltration and recharge into groundwater systems.

For deeper infiltration into the crust (Figure 2), the time scales are on the order of several decades to centuries, which will continuously reduce the surface water lost to the subsurface. It shows that on the decadal (or century) scales, water can infiltrate the crust below these dunes (within hours to days depending on dune depths) and continue to infiltrate while the ponded water increases. The time of infiltration to reach the water table is typically less in the heterogeneous crust (Figure 3c) compared to an equivalent homogeneous crust (Figure 3b). This occurs as the water table is within about 10%–20% of the surface-to-bedrock depth in most of highlands (Figures S3a and S3b in Supporting Information S1) where the porosity and hydraulic conductivity are higher than that for the homogeneous crust. However, the infiltration times for heterogeneous crust become longer than that of homogeneous crust when the water table depth is more than $\sim$55% of surface-to-bedrock depth, as the wetting front progressively slows with depth due to a decay in the porosity and conductivity (Figure S3c in Supporting Information S1). It shows that the heterogeneity of the crust will enhance the infiltration process and can transmit more water than that of the homogeneous case for shorter infiltration processes until the wetting front reaches the depth where the integrated hydraulic conductivity of the heterogeneous medium becomes smaller than the average hydraulic conductivity of the homogeneous medium (see Figure S2 in Supporting Information S1). This work can also be used to estimate the infiltration time of surface water basins, as they lose water to the subsurface over extended periods of time. In this case, until the wetting front reaches about 40% depth of the surface to bedrock depth ($\sim$4 km depth when the bedrock is 10 km below the surface), the heterogeneous medium causes more surface water loss to subsurface due to a higher infiltration rate (Figure S2a in Supporting Information S1), leads to a faster wetting front (Figure S2b in Supporting Information S1), and stores more water (Figure S2c in Supporting Information S1), than an equivalent homogeneous crust.

Infiltration may reduce the amount of runoff generated and therefore affect the total water available at the surface to be evaporated and absorbed into the climate system. The volume of water capable of being stored in the vadose zone has never been taken into account in the Mars' literature or in Mars groundwater modeling studies. The total amounts of water, expressed as the global equivalent layers (GEL) in the dry pore space without and with a water table (Figure 3a) are 199.18 and 82.28 m within the latitudinal band of $-45° < \theta < 45°$. Throughout Mars ($-90° < \theta < 90°$), the dry pore space without and with a water table (Figure 3a) comprises of a GEL of 1059.90 m and 350.83 m, respectively. The water budget in the vadose zone and the subsurface is very significant and will cause a significant error ($7.8 - 18.8\%$) if left unaccounted for. This also results in prolonged water sequestration for the duration of the time required to percolate downward. Ultimately, percolating water recharges the dynamically evolving deep crustal aquifer. The time delay between infiltration and recharge should be considered in existing groundwater models (e.g., Andrews-Hanna et al., 2008; Boatwright & Head, 2019; Hiatt et al., 2024).

This work assumes a ponded infiltration in a dry regolith due to excess precipitation when compared to the infiltration capacity f_c. As a result, it leads to faster wetting fronts in the regolith that fully saturate the regolith compared to unsaturated wetting fronts, leading to shorter infiltration times. However, the surface could remain unsaturated even after precipitation when $I < f_c$, leading to unsaturated wetting fronts that may completely saturate later while percolating in the subsurface with decaying porosity and permeability with depth (see Shadab & Hesse, 2022). The current model can be easily extended to include unsaturated wetting fronts using semi-analytic solutions provided in Shadab and Hesse (2022), which is a direction for future work. In addition, the initial saturation within the subsurface may further complicate the speeds of the wetting front. Furthermore, the model assumes that the near-surface and deep crust of early Mars were not affected by local heterogeneities such as impermeable layers of regolith or ice in pore spaces. If these layers are considered, the groundwater system may include confined aquifers below the impermeable layers (or unconfined if pores are not saturated to the elevation where the impermeable layers are formed) and unconfined above. The infiltration rates predicted in this work apply only to unconfined regions of the groundwater system. However, the location of the wetting front and thermal distribution could be used to estimate the formation of the ice layers due to the refreezing of percolating water. These pre-existing or newly formed ice layers would reduce the speed of the wetting front and increase the infiltration time (see Colbeck, 1972; Harlan, 1973; Shadab, Adhikari, et al., 2024; Shadab, Rutishauser, et al., 2024). Furthermore, refreezing processes may also lead to the formation of impermeable ice layers causing overland flow (e.g., Colbeck, 1977; Shadab, Rutishauser, et al., 2024), which are assumed to be laterally disconnected and thus neglected in the present analysis.

5. Conclusions

We investigated the dynamics of infiltration on early Mars near the surface, as well as deeper into the crust. These two spatiotemporal scales offer key insights into the partitioning of water in an integrated hydrological cycle on early Mars. Infiltration near the surface will lead to less ponded water in land evolution models, and this ultimately supports aeolian erosion and the geomorphology observed at the surface. We found that the infiltration rate decays with time as a result of the presence of vertical heterogeneity in the subsurface. For deeper infiltration into the Martian crust, percolation of the wetting front takes several decades to centuries to travel from the surface to the groundwater table. Only after infiltrated water has percolated down to the groundwater table will that water then recharge the groundwater system. During downward percolation, the accumulation of water in pore spaces has the ability to transiently sequester a significant portion of Mars' total available water budget. This has implications for the climate system, as conditions may be favorable for continued precipitation. However, transient sequestration may prevent water from evaporating and partitioning into the climate system for continued precipitation. Future work including dynamic infiltration in groundwater and land evolution models will help quantify the convolved effects of water partitioning in the climate system and the integrated hydrological cycle of early Mars.

Data Availability Statement

All codes corresponding to each figure are archived on Zenodo (Shadab et al., 2025) and provided on GitHub: https://github.com/mashadab/Infiltration-on-early-Mars.

Acknowledgments

M.A.S. acknowledges support from the University of Texas Institute for Geophysics (UTIG) through the Blue Sky Student Fellowship, and the Center for Planetary Systems Habitability (CPSH) through the Student Research Award in Planetary Habitability. Further, M.A.S. acknowledges the UT Austin Graduate School Fellowships. M.A.H. acknowledges support from NASA Emerging World Grant number 18−EW18_2 − 0027. E.H. acknowledges support from the Gale White Fellowship from the University of Texas Institute for Geophysics (UTIG), the Center for Planetary Systems Habitability (CPSH) through the Student Research Award in Planetary Habitability. The authors acknowledge the discussions with Timothy Goudge and Sean Gulick. Also, the authors thank Mackenzie Day and one anonymous reviewer whose insightful comments helped improve the quality of the work.

References

Andrews-Hanna, J. C., Phillips, R. J., & Zuber, M. T. (2007). Meridiani Planum and the global hydrology of Mars. *Nature*, *446*(7132), 163–166. https://doi.org/10.1038/nature05594

Andrews-Hanna, J. C., Zuber, M., & Banerdt, W. (2008). The Borealis basin and the origin of the Martian crustal dichotomy. *Nature*, *453*(7199), 1212–1215. https://doi.org/10.1038/nature07011

Andrews-Hanna, J. C., Zuber, M. T., Arvidson, R. E., & Wiseman, S. M. (2010). Early Mars hydrology: Meridiani playa deposits and the sedimentary record of Arabia Terra. *Journal of Geophysical Research E: Planets*, *115*(6), 1–22. https://doi.org/10.1029/2009JE003485

Beven, K. (1984). Infiltration into a class of vertically non-uniform soils. *Hydrological Sciences Journal*, *29*(4), 425–434. https://doi.org/10.1080/02626668409490960

Boatwright, B. D., & Head, J. W. (2019). Simulating early mars hydrology with the MARSSIM landform evolution model: New insights from an integrated system of precipitation, infiltration, and groundwater flow. *Planetary and Space Science*, *171*, 17–33. https://doi.org/10.1016/j.pss.2019.04.001

Cherry, J., & Freeze, A. (1979). *Groundwater* (1st ed.). Prentice Hall.

Clifford, S. M. (1993). A model for the hydrologic and climatic behavior of water on Mars. *Journal of Geophysical Research*, *98*(E6), 10973–11016. https://doi.org/10.1029/93je00225

Clifford, S. M., & Parker, T. (2001). The evolution of the Martian hydrosphere: Implications for the fate of a Primordial Ocean and the current state of the Northern Plains. *Icarus*, *154*(1), 40–79. https://doi.org/10.1006/icar.2001.6671

Colbeck, S. C. (1972). A theory of water percolation in snow. *Journal of Glaciology*, *11*(63), 369–385. https://doi.org/10.3189/S0022143000022346

Colbeck, S. C. (1977). Short-term forecasting of water run-off from snow and ice. *Journal of Glaciology*, *19*(81), 571–588. https://doi.org/10.3189/s0022143000215487

Ehlmann, B. L., Mustard, J. F., Murchie, S. L., Bibring, J.-P., Meunier, A., Fraeman, A. A., & Langevin, Y. (2011). Subsurface water and clay mineral formation during the early history of mars. *Nature*, *479*(7371), 53–60. https://doi.org/10.1038/nature10582

Fassett, C. I., & Head, J. W. (2008). Valley network-fed, open-basin lakes on Mars: Distribution and implications for Noachian surface and subsurface hydrology. *Icarus*, *198*(1), 37–56. https://doi.org/10.1016/j.icarus.2008.06.016

Gee, G. W., & Hillel, D. (1988). Groundwater recharge in arid regions: Review and critique of estimation methods. *Hydrological Processes*, *2*(3), 255–266. https://doi.org/10.1002/hyp.3360020306

Green, W., & Ampt, G. (1911). Studies on soil phyics. *The Journal of Agricultural Science*, *4*(1), 1–24. https://doi.org/10.1017/S0021859600001441

Grotzinger, J. P., Sumner, D. Y., Kah, L., Stack, K., Gupta, S., Edgar, L., et al. (2014). A habitable fluvio-lacustrine environment at Yellowknife Bay, Gale Crater, Mars. *Science*, *343*(6169), 1242777. https://doi.org/10.1126/science.1242777

Haberle, R. M., Clancy, R. T., Forget, F., Smith, M. D., & Zurek, R. W. (2017). *The atmosphere and climate of Mars*. Cambridge University Press.

Hanna, J. C., & Phillips, R. J. (2005). Hydrological modeling of the Martian crust with application to the pressurization of aquifers. *Journal of Geophysical Research: Planets*, *110*(1), 1–19. https://doi.org/10.1029/2004JE002330

Harlan, R. (1973). Analysis of coupled heat-fluid transport in partially frozen soil. *Water Resources Research*, *9*(5), 1314–1323. https://doi.org/10.1029/wr009i005p01314

Hiatt, E., Shadab, M. A., Gulick, S. P., Goudge, T. A., & Hesse, M. A. (2024). Limited recharge of the southern highlands aquifer on early mars. *Icarus*, *408*, 115774. https://doi.org/10.1016/j.icarus.2023.115774

Horvath, D. G., & Andrews-Hanna, J. C. (2017). Reconstructing the past climate at Gale Crater, Mars, from hydrological modeling of late-stage lakes. *Geophysical Research Letters*, *44*(16), 8196–8204. https://doi.org/10.1002/2017gl074654

Horvath, D. G., & Andrews-Hanna, J. C. (2021). The hydrology and climate of Mars during the sedimentary infilling of Gale crater. *Earth and Planetary Science Letters*, *568*, 117032. https://doi.org/10.1016/j.epsl.2021.117032

Howard, A. D. (1994). A detachment-limited model of drainage basin evolution. *Water Resources Research*, *30*(7), 2261–2285. https://doi.org/10.1029/94wr00757

Hynek, B., Beach, M., & Hoke, M. (2010). Updated global map of Martian valley networks and implications for climate and hydrologic processes. *Journal of Geophysical Research*, *115*(E9), E09008. https://doi.org/10.1029/2009JE003548

Jarihani, A. A., Larsen, J. R., Callow, J. N., McVicar, T. R., & Johansen, K. (2015). Where does all the water go? Partitioning water transmission losses in a data-sparse, multi-channel and low-gradient dryland river system using modelling and remote sensing. *Journal of Hydrology*, *529*, 1511–1529. https://doi.org/10.1016/j.jhydrol.2015.08.030

Kale, R., & Sahoo, B. (2011). Green-ampt infiltration models for varied field conditions: A revisit. *Water Resources Management*, *25*(14), 3505–3536. https://doi.org/10.1007/s11269-011-9868-0

Luo, W., & Howard, A. (2008). Computer simulation of the role of groundwater seepage in forming Martian valley networks. *Journal of Geophysical Research*, *113*(E5), E05002. https://doi.org/10.1029/2007JE002981

Malin, M. C., & Edgett, K. S. (2000). Evidence for recent groundwater seepage and surface runoff on Mars. *Science*, *288*(5475), 2330–2335. https://doi.org/10.1126/science.288.5475.2330

Manga, M., & Wright, V. (2021). No cryosphere-confined aquifer below InSight on Mars. *Geophysical Research Letters*, *48*(8). https://doi.org/10.1029/2021GL093127

Manning, C. E., & Ingebritsen, S. E. (1999). Permeability of the continental crust: Implications of geothermal data and metamorphic systems. *Reviews of Geophysics*, *37*(1), 127–150. https://doi.org/10.1029/1998rg900002

Mathias, S. A., Reaney, S. M., & Kenabatho, P. K. (2021). Transmission loss estimation for ephemeral sand rivers in southern Africa. *Journal of Hydrology*, *600*, 126487. https://doi.org/10.1016/j.jhydrol.2021.126487

Mein, R., & Larson, C. (1973). Modeling infiltration during a steady rain. *Water Resources Research*, *9*(2), 384–394. https://doi.org/10.1029/WR009i002p00384

Pelletier, J. D. (2008). Quantitative modeling of earth surface processes.

Salese, F., Kleinhans, M. G., Mangold, N., Ansan, V., McMahon, W., De Haas, T., & Dromart, G. (2020). Estimated minimum life span of the jezero fluvial delta (Mars). *Astrobiology*, *20*(8), 977–993. https://doi.org/10.1089/ast.2020.2228

Salese, F., Pondrelli, M., Neeseman, A., Schmidt, G., & Ori, G. G. (2019). Geological evidence of planet-wide groundwater system on Mars. *Journal of Geophysical Research: Planets*, *124*(2), 374–395. https://doi.org/10.1029/2018JE005802

Scanlon, B. R., Keese, K. E., Flint, A. L., Flint, L. E., Gaye, C. B., Edmunds, W. M., & Simmers, I. (2006). Global synthesis of groundwater recharge in semiarid and arid regions. *Hydrological Processes: An International Journal*, *20*(15), 3335–3370. https://doi.org/10.1002/hyp.6335

Selker, J. S., Duan, J., & Parlange, J.-Y. (1999). Green and Ampt infiltration into soils of variable pore size with depth. *Water Resources Research*, *35*(5), 1685–1688. https://doi.org/10.1029/1999WR900008

Shadab, M. A., Adhikari, S., Rutishauser, A., Grima, C., & Hesse, M. A. (2024). A mechanism for ice layer formation in glacial firn. *Geophysical Research Letters*, *51*(15), e2024GL109893. https://doi.org/10.1029/2024gl109893

Shadab, M. A., & Hesse, M. A. (2022a). Analysis of gravity-driven infiltration with the development of a saturated region. *Water Resources Research*, *1*(1), 1. https://doi.org/10.1029/2022wr032963

Shadab, M. A., & Hesse, M. A. (2022b). *mashadab/hyperbolic-infiltration-theory: v1.0*. Zenodo. https://doi.org/10.5281/zenodo.7080194

Shadab, M. A., Hiatt, E., Bahia, R. S., Bohacek, E. V., Steinmann, V., & Hesse, M. A. (2025). mashadab/infiltration-on-early-mars: v1.0.1 (v1.0.1) [software]. *Zenodo*. https://doi.org/10.5281/zenodo.14742437

Shadab, M. A., Hiatt, E., & Hesse, M. (2023). Investigating groundwater dynamics and residence times on early mars using unconfined aquifer model with vertical heterogeneity. *LPI Contribution*, *2806*, 1736.

Shadab, M. A., Rutishauser, A., Grima, C., & Hesse, M. A. (2024). A unified kinematic wave theory for melt infiltration into firn. arXiv preprint arXiv:2403.15996.

Smith, D. E., Zuber, M. T., Frey, H. V., Garvin, J. B., Head, J. W., Muhleman, D. O., et al. (2001). Mars orbiter laser altimeter: Experiment summary after the first year of global mapping of mars. *Journal of Geophysical Research*, *106*(E10), 23689–23722. https://doi.org/10.1029/2000je001364

Squyres, S. W., Grotzinger, J. P., Arvidson, R. E., Bell, J. F., III., Calvin, W., Christensen, P. R., et al. (2004). In situ evidence for an ancient aqueous environment at Meridiani Planum, Mars. *Science*, *306*(5702), 1709–1714. https://doi.org/10.1126/science.1104559

Tucker, G. E., & Hancock, G. R. (2010). Modelling landscape evolution. *Earth Surface Processes and Landforms*, *35*(1), 28–50. https://doi.org/10.1002/esp.1952

Wordsworth, R. D. (2016). The climate of early Mars. *Annual Review of Earth and Planetary Sciences*, *44*(1), 381–408. https://doi.org/10.1146/annurev-earth-060115-012355